An algorithm for robust and efficient location of T-wave ends in electrocardiogram

Qinghua Zhang, Alfredo Illanes Manriquez, Claire Médigue, Yves Papelier, Michel Sorine

I R I S A
INSTITUT DE RECHERCHE EN INFORMATIQUE ET SYSTÈMES ALÉATOIRES

PUBLICATION
INTERNE
N° 1744

AN ALGORITHM FOR ROBUST AND EFFICIENT LOCATION OF T-WAVE ENDS IN ELECTROCARDIOGRAM

QINGHUA ZHANG, ALFREDO ILLANES MANRIQUEZ, CLAIRE MEDIGUE, YVES PAPELIER AND MICHEL SORINE

ISSN 1166-8687

IRISA
CAMPUS UNIVERSITAIRE DE BEAULIEU - 35042 RENNES CEDEX - FRANCE

IRISA

INSTITUT DE RECHERCHE EN INFORMATIQUE ET SYSTÈMES ALÉATOIRES
Campus de Beaulieu – 35042 Rennes Cedex – France
Tél. : (33) 02 99 84 71 00 – Fax : (33) 02 99 84 71 71
http://www.irisa.fr

An algorithm for robust and efficient location of T-wave ends in electrocardiogram

Qinghua ZHANG*, Alfredo ILLANES MANRIQUEZ, Claire MEDIGUE, Yves PAPELIER** and Michel SORINE

Systèmes biologiques
Projet SOSSO2

Publication interne n ° 1744 — Octobre 2005 — 19 pages

Abstract: Computer-aided analysis of electrocardiogram (ECG) is widely used in cardiac disease diagnosis. The purpose of this paper is to propose a new algorithm for T-wave end location, which is known to be the most difficult one among ECG wave form detection and location problems. The proposed algorithm mainly consists of the computation of an indicator related to the area covered by the T-wave curve and delimited in a special manner. Based on simple assumptions, essentially on the concavity of the T-wave form, it is formally proved that the maximum of the computed indicator inside each cardiac cycle coincides with the T-wave end. Moreover, the algorithm is robust to measurement noise, to wave form morphological variations and to baseline wander. It is also computationally very simple: the main computation can be implemented as a simple finite impulse response (FIR) filter. When evaluated with the PhysioNet QT database in terms of the mean and the standard deviation of the T-wave end location errors, the proposed algorithm outperforms the other algorithms evaluated with the same data base, according to the most recent available publications up to our knowledge.

Key-words: electrocardiogram (ECG), T-wave end location, signal processing

(Résumé : tsvp)

* Email: zhang@irisa.fr
** Y. Papelier is with Hôpital Antoine-Béclère, whereas the other authors are all with INRIA.

Centre National de la Recherche Scientifique
(UMR 6074) Université de Rennes 1 – Insa de Rennes

Institut National de Recherche en Informatique
et en Automatique – unité de recherche de Rennes

Un algorithme pour la localisation robuste et efficace de fins d'ondes T dans l'électrocardiogramme

Résumé : L'analyse de l'électrocardiogramme (ECG) assistée par l'ordinateur est largement utilisée en diagnostic de maladies cardiaques. Le but de cet article est de proposer un nouveau algorithme pour la localisation de fins d'ondes T, connu d'être le plus difficile des problèmes concernant la détection et localisation d'ondes dans l'ECG. L'algorithme proposé consiste principalement à calculer un indicateur lié à la surface couverte par l'onde T délimitée d'une manière spéciale. Sous des hypothèses simples, principalement sur la concavité de l'onde T, il est démontré que le maximum de l'indicateur calculé dans chaque cycle cardiaque coïncide avec la fin de l'onde T. En plus, l'algorithme est robuste au bruit de mesure, aux variations morphologiques et à la dérive de la ligne de base. Le calcul numérique est très simple : le calcul principal peut être implémenté sous forme d'un filtre à réponse impulsionnelle finie. Quand cet algorithme est évalué sur la base de données QT de PhysioNet en termes de la moyenne et l'écart type des erreurs de localisation de l'onde T, il obtient de meilleurs résultats par rapport à d'autres algorithmes évalués avec la même base de données, d'après les publications les plus récentes à notre connaissance.

Mots clés : electrocardiogramme (ECG), localisation de fins d'ondes T, traitement de signal

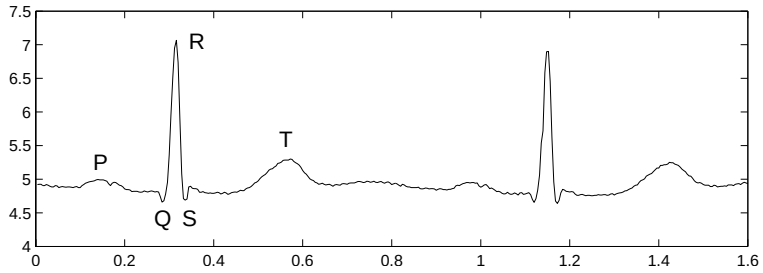

Figure 1: ECG signal and P-Q-R-S-T wave forms

1 Introduction

Automatic processing of electrocardiogram (ECG) has been one of the earliest applications of modern digital computers. In this vast field, automatic detection of wave forms in ECG signals is still an active research topic, as demonstrated by recent publications (Kohler et al., 2002; Strumillo, 2002; Martínez et al., 2004; Last et al., 2004). In an ECG signal, each cardiac cycle is typically characterized by successive wave forms, known as P-wave, QRS-complex and T-wave among the most important ones, as illustrated in Figure 1. The detection of these wave forms and the location of their boundaries provide important information about cardiac dysfunctions. For instance, the QT interval is a traditional measurement for the diagnosis of ventricular arrhythmia (Schuartz and Wolf, 1978; Moss et al., 1985). Because of the great morphological variations in ECG signals, it is difficult to design automatic and widely applicable algorithms. This difficulty partly explains the continuous efforts made by researchers on ECG signal processing.

It is widely acknowledged that T-wave end location is the most difficult one among wave form boundary location problems, due to the slow transition in the signal around each T-wave end, eventually corrupted by noise. It is not the purpose of this paper to review the existing vast literature. However, some typical methods for T-wave end location are shortly recalled in the following in order to contrast the novelty of the algorithm proposed in this paper.

It is generally considered that T-wave end is related to some sudden change in the variations of the ECG signal. Therefore, various methods have been proposed based on numerical differentiation of ECG signal, since the time derivative is an indicator of signal variation. For instance, in (Laguna et al., 1994) T-wave end location is based on linear derivative filters, and in (Martínez et al., 2004) wavelets are used to estimate derivatives at different scales. Some similar work based on wavelet transforms has been presented in (Li et al., 1995). The advantage of this method is its robustness to wave form morphological variations. Its drawback is related to numerical differentiation which is generally known to be noise-sensitive. Usually, low-pass smoothing filters are also used in order to limit noise sensitivity.

Pattern recognition techniques have been widely applied to ECG processing. In such an approach, the basic idea for wave form detection is to first build a template of the form to be detected and then to locate the corresponding form in the processed signal by looking for signal segments highly correlated with the template (Abboud and Sadeh, 1984; Lindecrantz and Lilja, 1988; Last et al., 2004). Such methods have the advantage to be robust to measurement noise. However, due to the large morphological variations in wave forms, it seems not reasonable to build a "universal" template to cover all different situations. Building a specific template for each particular case may need the intervention of human experts.

Mathematical models of ECG can also be applied to wave form detection (Malik and Camm, 1989; Padrini et al., 1995). In (Vila et al., 2000), the T-wave and U-wave are formulated as the differences of activation potentials described with a simple parametric model. The model is fitted to ECG signal segments by tuning the model parameters through a numerical optimization procedure. The fitted model is then used to locate wave form boundaries. This method is in principle robust to noise and can be adapted to various morphological forms, but it is highly expensive in terms of numerical computation, and may be sensitive to parameter initializations.

The purpose of this paper is to propose a new algorithm for the location of T-wave end. Its most remarkable difference from existing algorithms is its consistency proof based on simple assumptions, essentially the concavity of the T-wave form. Moreover, it has the following advantages:

- it is robust to measurement noise, since the computation in the algorithm mainly consists of an integration operation;
- it is robust to wave form morphological variations and to baseline wander, since the consistency of the algorithm is essentially based on the assumption of T-wave concavity, and *no* threshold is needed to determine T-wave end location;
- it is computationally very simple: the main computation is an integration operation over a sliding window and can be implemented as a simple finite impulse response (FIR) filter.

When evaluated with manually annotated ECG signals of the QT database (Laguna et al., 1997) available on the PhysioNet web site (Goldberger et al., 2000), the proposed algorithm outperforms the other algorithms evaluated with the same data base, according to the most recent available publications up to our knowledge. These numerical results can be reproduced with the Matlab package (Zhang, 2005) which can be downloaded at http://www.irisa.fr/sosso/zhang/biomedical/.

Notice that this paper considers only T-wave end location. For this purpose, the QRS complex detection needs to be first performed in order to delimit an interval containing the T-wave. Because the QRS complex is the easiest wave form to be detected, no further discussion on this subject is pursued in this paper.

The paper is organized as follows. The proposed algorithm is first heuristically introduced in Section 2.1, its consistency is then analyzed in Section 2.2. The classification of T-wave

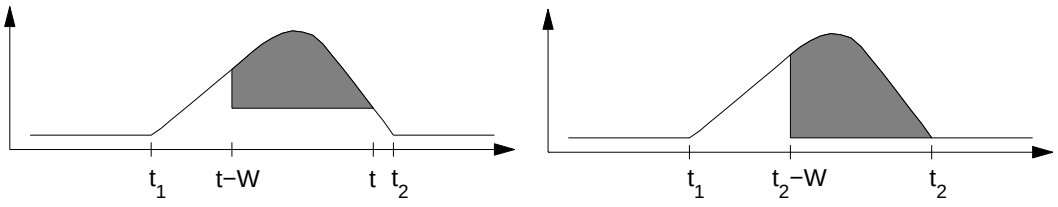

Figure 2: Sliding window of size W for the computation of $A(t)$

morphological forms is discussed in Section 2.3. The complete algorithm in discrete time is formulated in Section 2.4. The algorithm performance is then evaluated in Section 3 with the PhysioNet QT database. Finally, some concluding remarks are drawn in Section 4.

2 The proposed algorithm and its consistency analysis

2.1 Notations and heuristics

In order to concentrate the presentation to the main elements of the proposed algorithm, let us first consider positive T-waves (as those shown in Figure 1). The other T-wave morphologies will be treated similarly later in this paper.

For the convenience of presentation, the ECG signal is first considered as a continuous function of the time t, denote by $s(t)$. Nevertheless, the full algorithm will be reformulated in Section 2.4 for ECG signals sampled at discrete time instants.

Based on QRS-complex detection (this task can be accomplished with any well established QRS detection method; see, *e.g.*, (Kohler et al., 2002)), for each cardiac cycle, a interval $[t_a, t_b]$ is roughly delimited so that the T-wave end is inside this interval, with no overlap with the other wave forms (QRS and P). The following presentation assumes that such an interval is already chosen for each cardiac cycle.

Throughout this paper, the time instants corresponding to the beginning and the end of a T-wave are respectively denoted by t_1 and t_2. The T-wave length, denoted by $L = t_1 - t_2$, is generally an unknown value.

The proposed algorithm mainly consists of the computation of an indicator $A(t)$ which reaches its maximum value when $t = t_2$. It is computed mainly through an integration operation in a sliding window. The window size W should be chosen such that $0 < W < L$. It is possible to choose such a value with some rough knowledge on L. At each time instant t, define the indicator

$$A(t) = \int_{t-W}^{t} [s(\tau) - s(t)] d\tau \tag{1}$$

which can be understood as the area in the interval $[t{-}W, t]$ under the signal $s(t)$, but above the horizontal line crossing the point $s(t)$, as illustrated in Figure 2(a).

Remark 1 For presentation convenience, and by abuse of language, the term "area $A(t)$" will mean *both* the value defined by the integral in (1) and the corresponding geometric object. For instance, with its second meaning, the *left side edge* and the *bottom line* of the area $A(t)$ can be talked about. □

Before the detailed proof presented later, let us first intuitively explain why the area $A(t)$ reaches its maximum value when $t = t_2$. From this position, as illustrated in Figure 2(b), when the window (of size $W < L$) is moved to the right side, part of the window is covering the baseline instead of the T-wave, then $A(t)$ decreases. When the window is moved to the left side, the bottom line of the area moves up with the value of $s(t)$, then the area $A(t)$ also decreases. Therefore, intuitively, the T-wave end can be located by looking for the time t maximizing $A(t)$.

Let us introduce some other useful notations: the time instant when the T-wave reaches its maximum

$$t_{\text{top}} = \arg \max_{t \in [t_1, t_2]} s(t) \tag{2}$$

the left edge height of the area $A(t)$

$$h(t) = s(t - W) - s(t) \tag{3}$$

and the maximum height of the area $A(t_2)$:

$$h_{\max}(t_2) = \max_{t \in [t_2 - W,\, t_2]} [s(t) - s(t_2)] \tag{4}$$

2.2 Assumptions and consistency analysis

Assumption 1 *A T-wave is a differentiable* concave *function of the time in the interval $[t_1, t_2]$. It is followed by a straight-line in the interval $[t_2, t_b]$ (a piece of the baseline).*

This assumption is only approximatively true, since a typical T-wave may not be concave in the neighborhoods of t_1 and t_2 and the baseline following the T-wave may not strictly form a straight-line. However, despite this approximation, the resulting algorithm proposed in this paper produces accurate results when evaluated with the PhysioNet QT database, as shown in Section 3.

Assumption 2 *If the straight-line segment of $s(t)$ in the interval $[t_2, t_b]$ has a negative slope K, then it is weak enough such that $|K| \leq h(t)/W$ for any $t \in [t_2, t_b]$. Graphically, this assumptions means that the left extension of this straight-line intersects with the left edge of the area $A(t)$ (see Figure 4(c)).*

Remark that the straight-line in the interval $[t_2, t_b]$ may have a positive, zero, or negative slope. The restriction on its slope applies only in the negative slope case.

Assumption 3 *The segment of the signal in the interval* $[t_a - W,\, t_1]$ *preceding the T-wave is not necessarily a straight-line, but is upper bounded such that*

$$s(t) \leq s(t_{top}) \tag{5}$$

and satisfies the Lipschitz condition

$$|s(t) - s(\tau)| \leq \frac{h_{max}(t_2)}{W}|t - \tau| \quad \textit{for any} \quad t, \tau \in [t_a - W,\, t_1] \tag{6}$$

Remind that the interval $[t_a, t_b]$ is assumed to contain the T-wave end instant t_2, not the entire T-wave interval $[t_1, t_2]$.

Now it is ready to establish the main result for T-wave end location.

Proposition 1 *Under Assumptions 1, 2 and 3, the T-wave end satisfies the property*

$$t_2 = \arg \max_{t \in [t_a, t_b]} A(t)$$

Proof. Depending on the size of $[t_a, t_b]$, either $t_a < t_{\text{top}}$ or $t_a \geq t_{\text{top}}$ is true. The following proof considers only the situation $t_a < t_{\text{top}}$ as illustrated in Figure 3. Whenever $t_a \geq t_{\text{top}}$ happens, t_a can be simply replaced, in the following proof, by $t'_a = t_{\text{top}} - \varepsilon$ with some small value $\varepsilon > 0$. If t_2 maximizes $A(t)$ within $[t'_a, t_b]$, the maximization holds also for $[t_a, t_b] \subset [t'_a, t_b]$.

In order to prove that $A(t)$ reaches its maximum value within $[t_a, t_b]$ at $t = t_2$, it will be shown that $A(t) < A(t_2)$ for any $t \in [t_a, t_b]$ and $t \neq t_2$. For this purpose, the interval $[t_a, t_b]$ is divided into 3 pieces, separated by t_{top} and t_2. Each case with t falling into one of these 3 sub-intervals are considered in detail.

Case 1, $t \in [t_{\text{top}}, t_2)$.

This is the middle sub-interval. Consider any value of $t \in [t_{\text{top}}, t_2)$. From this position, move the sliding window an infinitesimal distance $dt > 0$ to the right (such that $t + dt \leq t_2$). Accordingly, the bottom line of the area $A(t)$ is moved down a distance $ds > 0$. See Figure 3 where the dashed lines illustrate the border of the area $A(t + dt)$ after the movement.

Denote with $s'(t)$ the derivative of $s(t)$, then

$$ds = |s'(t)|dt$$

where the absolute value $|s'(t)|$ is used because dt and ds have been taken as positive values for a simple graphical interpretation of the proof. After this movement, the area is decreased at its left edge, but increased at its bottom. The total area increment is

$$dA(t) = W ds - h(t)dt$$

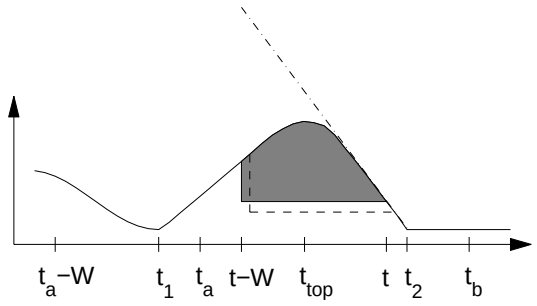

Figure 3: Illustration of $A(t)$ in case 1.

Then

$$\begin{aligned} dA(t) &= W|s'(t)|dt - h(t)dt \\ &= W\left(|s'(t)| - \frac{h(t)}{W}\right)dt \end{aligned}$$

Because $s(t)$ is a concave function inside the interval $[t_1, t_2]$, the tangent line of the T-wave stays above the T-wave, as illustrated in Figure 3 with the dotted line. If $t - W \geq t_1$, the slope of the tangent line $s'(t)$ satisfies the inequality $|s'(t)| > \frac{h(t)}{W}$. If $t - W < t_1$, by Assumption 3, $s(t - W) < s(t_{\text{top}})$, then the inequality $|s'(t)| > \frac{h(t)}{W}$ also holds. It follows that $dA(t) > 0$.

Notice that $dA(t) > 0$ has been proved for the movement to the *right* from *any* position $t \in [t_{\text{top}}, t_2)$. In other words, for *any* $t \in [t_{\text{top}}, t_2)$, when the sliding window is slightly moved to the right, the area $A(t)$ increases. It then follows by continuity of $A(t)$ that $A(t) < A(t_2)$ for any $t \in [t_{\text{top}}, t_2)$.

Case 2, $t \in (t_2, t_b]$.

In this case, three sub-cases have to be considered, according to the sign of the slope of the straight-line ECG segment in the interval $[t_2, t_b]$.

If the slope in the interval $[t_2, t_b]$ is zero (horizontal baseline), as illustrated in Figure 4(a), then the area $A(t)$ decreases when it is moved to the right side, since the area at the right end disappears, and the area at the left end decreases.

If the slope is positive (see Figure 4(b)), then the part of the area $A(t)$ below $s(t)$ (the positive part of A(t), illustrated in Figure 4(b) with the gray area) is certainly smaller than $A(t_2)$, since from the t_2 position to the current position, the left edge of this part has been moved to the right and the bottom edge has been moved up. Moreover, there is also a negative part of $A(t)$ (illustrated in Figure 4(b) with the white area). Therefore, $A(t) < A(t_2)$ certainly holds.

If the slope is negative, as illustrated in Figure 4(c), the proof is similar to that of Case 1. For any $t \in [t_2, t_b)$, move the sliding window an infinitesimal distance $dt > 0$ to the right.

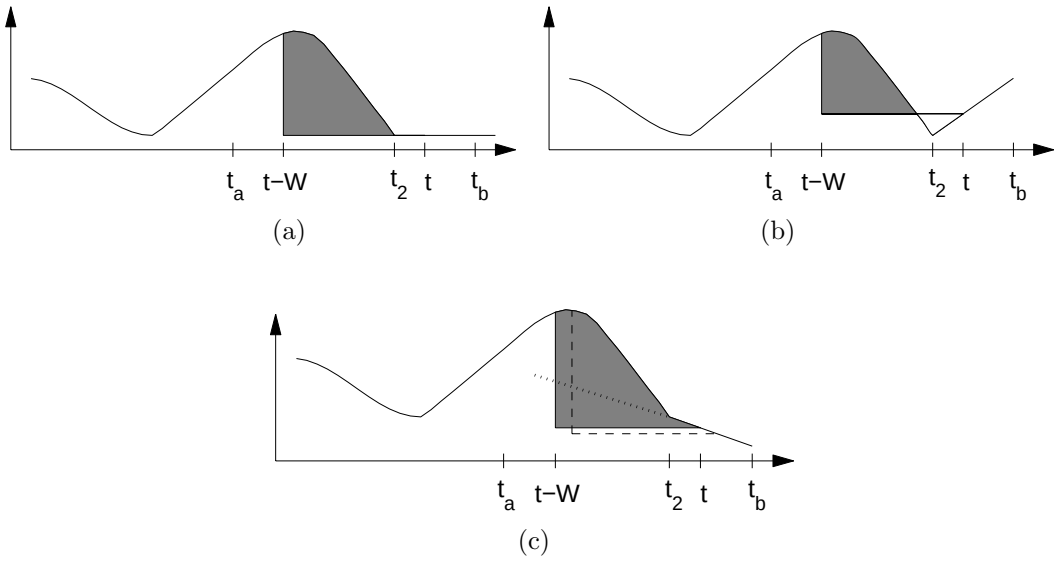

Figure 4: Illustrations of $A(t)$ in case 2.

Accordingly, $s(t)$ is moved down of the distance $ds = |s'(t)|dt$. Once again, the absolute value $|s'(t)|$ is used for positive values dt and ds. Then the area increment caused by the movement is

$$\begin{aligned} dA(t) &= W ds - h(t)dt \\ &= W\left(|s'(t)| - \frac{h(t)}{W}\right) dt \end{aligned}$$

According to Assumption 2, $|s'(t)| < h(t)/W$, therefore $dA(t) < 0$. Notice that this result holds for any $t \in [t_2, t_b)$, it then follows that $A(t) < A(t_2)$ for any $t \in (t_2, t_b]$.

Case 3, $t \in [t_a, t_{\text{top}}]$. In this case, three sub-cases should also be considered, depending on the position of t_1 with respect to the interval $[t - W, t]$.

First consider the sub-case of $t_1 < t - W$, as illustrated in Figure 5-(a). The window $[t - W, t]$ is then entirely inside the increasing side of the T-wave, *i.e.*, $[t - W, t] \subset [t_1, t_{\text{top}}]$. Due to the concavity of the T-wave, $s(\tau) - s(t) < 0$ for any $\tau \in [t - W, t)$. Therefore $A(t) < 0$ following its definition. It is then trivial to show $A(t) < 0 < A(t_2)$.

Now let us consider the sub-case of $t_1 \in [t - W, t]$, as illustrated in Figure 5-(b).

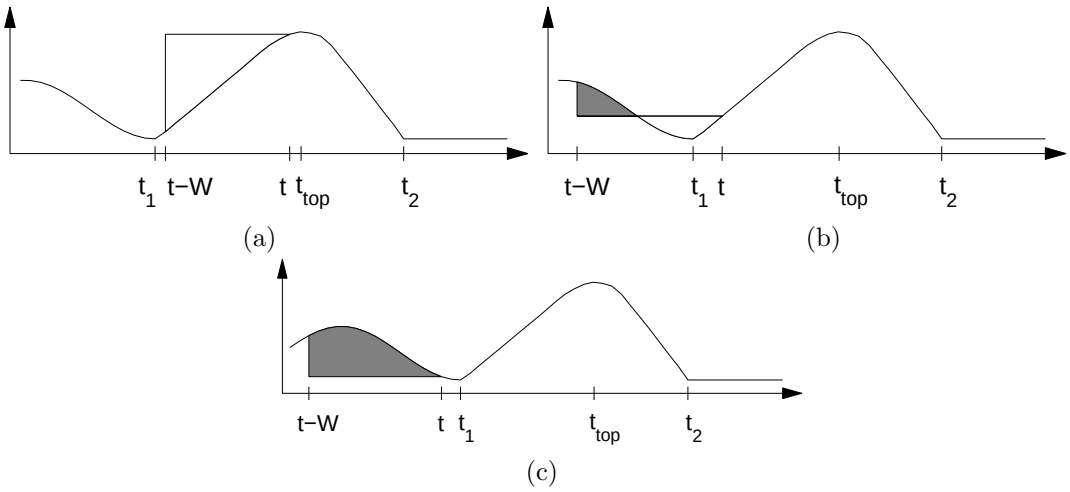

Figure 5: Illustration of $A(t)$ in case 3.

Define the notations:

$$B(t) = \int_{t-W}^{t_1} [s(\tau) - s(t)]d\tau$$
$$s_{\min} = \min_{\tau \in [t-W, t_1]} s(\tau)$$

Notice that

$$A(t) = B(t) + \int_{t_1}^{t} [s(\tau) - s(t)]d\tau$$

Because of the concavity of the T-wave, $s(\tau) - s(t) < 0$ for all $\tau \in [t_1, t)$, therefore $A(t) < B(t)$. It will be shown in the following that $B(t) < A(t_2)$.

Because of the T-wave concavity, $s(t_1) \leq s(t)$, therefore $s_{\min} \leq s(t_1) \leq s(t)$. Then

$$\begin{aligned} B(t) &= \int_{t-W}^{t_1} [s(\tau) - s(t)]d\tau \\ &\leq \int_{t-W}^{t_1} [s(\tau) - s_{\min}]d\tau \end{aligned}$$

The application of Lemma 1 (see the Appendix of this paper) leads to

$$B(t) \leq \frac{1}{2} \frac{h_{\max}(t_2)}{W} [t_1 - (t - W)]^2$$

where the Lipschitz constant $h_{\max}(t_2)/W$ assumed in Assumption 3 has been used.

For the current case $t_1 \in [t-W, t]$, clearly $[t_1 - (t-W)]^2 \leq W^2$. Then

$$B(t) \leq \frac{1}{2} h_{\max}(t_2) W$$

The concavity of the T-wave implies that $A(t_2) > \frac{1}{2} h_{\max}(t_2) W$. Therefore,

$$A(t) \leq B(t) < A(t_2)$$

Now let us consider the last sub-case $t_1 > t$ as illustrated in Figure 5-(c). First notice that the interval $[t-W, t]$ is covered by Assumption 3, since $[t-W, t] \subset [t_a - W, t_1]$. Then the proof is similar to that of the previous sub-case: Assumption 3 and Lemma 1 lead to

$$\begin{aligned} A(t) &= \int_{t-W}^{t} [s(\tau) - s(t)] d\tau \\ &\leq \frac{1}{2} h_{\max}(t_2) W \\ &< A(t_2) \end{aligned}$$

It is then established that $A(t) < A(t_2)$ for all $t \in [t_a, t_{\text{top}}]$.

Finally it is concluded that Proposition 1 holds in all the possible cases. □

2.3 Other T-wave morphological forms

Remind that Proposition 1 has been formulated for positive T-waves. Following (Martínez et al., 2004), T-wave morphologies can be classified as positive, negative, biphasic (positive-negative or negative-positive), ascending only, and descending only.

For negative T-waves, the same algorithm can be applied to $-s(t)$ instead of $s(t)$, or equivalently, the minimum of $A(t)$ is searched for instead of its maximum.

For biphasic negative-positive T-waves, let t_1 be the inflexion point inside the T-wave so that $s(t)$ is concave in the interval $[t_1, t_2]$. Biphasic positive-negative T-waves can be handled similarly.

For descending only T-waves, let $t_1 = t_2 - L$ for some appropriate value L. The ascending only case is similarly handled.

Typically, a T-wave end location algorithm has to first figure out the morphology of a T-wave before determining the wave end location. For the algorithm proposed in this paper, it is important to know if the end of a T-wave is located after a *descending* or an *ascending* edge of the T-wave. If it is descending, then Proposition 1 applies. If it is ascending, then Proposition 1 applies to $-s(t)$ instead of the signal $s(t)$ itself.

Since the T-wave morphology is *a priori* not known, a simple solution would be to search for the maximum absolute value $|A(t)|$ for T-wave end location. However, for biphasic T-waves, the wave end does not necessarily correspond to the maximum of $|A(t)|$. Therefore,

continuous time	$s(t)$	$A(t)$	W	t_a	t_b	t_2
discrete time	s_k	A_k	w	k_a	k_b	k_2

Table 1: Notation correspondence between continuous time and discrete time

the following simple rule is adopted. Search for the instants t' and t'' respectively maximizing and minimizing $A(t)$. If $A(t')$ and $A(t'')$ have comparable absolute values (decided based on a threshold value), then the T-wave is considered as biphasic, and the latest of the two instants t and t'' is taken as the location of the T-wave end. Otherwise, the largest absolute value $|A(t')|$ or $|A(t'')|$ corresponds to the T-wave end.

Remark 2 Better result can be obtained if the sliding window size W is specialized to each T-wave morphology. However, due to the robustness of the algorithm to parameter tuning, in this paper the same value of W is used for all the T-wave morphologies. □

2.4 Algorithm in discrete time

In practice, ECG signals are typically sampled at discrete time instants before being processed with a digital computer. Assume that the signal is sampled at a constant period Δ, and with $s_k = s(k\Delta)$ being the k-th sampled signal value. Then the ECG signal becomes a sequence of values s_k with $k = 1, 2, \ldots$. Accordingly, the definition of $A(t)$ is reformulated in discrete time as

$$A_k = \sum_{j=k-w+1}^{k} (s_j - s_k)$$

where w is the sliding window size in discrete time. In order to reduce of the effect of measurement noise, in the above formula it is better to replace s_k by $\bar{s}_k$, the mean value of the signal in a small window around k.

Some other notations already introduced in continuous time are also translated into discrete time, as summarized in Table 1.

A QRS-complex detection algorithm is first applied to detect R-peaks, with R_i denoting the i-th detected R-peak (discrete time) instant. Inside each detected RR interval, two discrete time instants k_a and k_b are chosen to confine the T-wave end search. Then for each instant k between k_a and k_b, the value of A_k is computed and the T-wave end is located at the value of k maximizing or minimizing A_k, as summarized in the following.

Algorithm summary

1. Choose the sliding window size w and the smoothing window size $p << w$. Choose also a threshold $\lambda > 1$ for T-wave morphology classification.
2. Read two successively detected R-peak instants R_i and R_{i+1}.
3. Choose the values of k_a, k_b between R_i and R_{i+1} to confine the T-wave end search.

4. For each instant $k = k_a, k_a + 1, \ldots, k_b$, compute

$$\bar{s}_k = \frac{1}{2p+1} \sum_{j=k-p}^{k+p} s_j$$

$$A_k = \sum_{j=k-w+1}^{k} (s_j - \bar{s}_k)$$

5. Find

$$k' = \arg \max_{k_a \le k \le k_b} A_k$$

$$k'' = \arg \min_{k_a \le k \le k_b} A_k$$

6. If

$$\frac{1}{\lambda} < \frac{|A_{k'}|}{|A_{k''}|} < \lambda$$

then the T-wave end in the current RR interval is located at

$$k_2 = \max(k', k'')$$

otherwise,

$$k_2 = \arg \max_{k \in \{k', k''\}} |A_k|$$

7. Increase i by one and go back to step 2.

Remark 3 The main part of this algorithm, the computation of A_k, is in fact a linear combination of the signal values from s_{k-w+1} to s_{k+p}. It can thus be simply implemented as a finite impulse response (FIR) filter. □

The choice of k_a, k_b in each RR interval has an important influence on the result of T-wave end detection. They should define an interval large enough to contain the T-wave end, and small enough in order to avoid overlap with the other wave forms. As an example, the rule for choosing k_a, k_b when the algorithm is applied to the PhysioNet QT database will be given in the next section.

For the algorithm presented above, it is assumed that a T-wave is present in each cardiac cycle. In some situations, the signal segment corresponding to a T-wave is so weak that the T-wave end cannot be correctly detected. Such situations can be identified with the aid of the maximum absolute value $|A_k|$ compared with a threshold. The value of this threshold has to be determined experimentally.

3 Evaluation with manually annotated ECG signals

The PhysioNet QT database (Laguna et al., 1997) has been built by researchers to serve as a reference for the validation and comparison of ECG processing algorithms. The signals in this database have been manually annotated by cardiologist experts for various events. Only the T-wave end annotations are used in this paper. In 105 records, a total of 3542 T-wave ends have been annotated by one cardiologist, and 402 T-wave ends in 11 records have been annotated by another cardiologist. Each record consists of two leads of 15 minutes ECG signals sampled at 250 Hz.

The signals are first filtered to reduce baseline wander before the application of the proposed detection algorithm. For simplicity, the Fast Fourier Transform (FFT) of each signal is first computed and then the frequency components below 0.5 Hz are truncated before the inverse FFT is computed. Filtering is not really necessary for the QT database, as will be shown by the result without filtering. However, filtering is generally recommended to prevent bad surprises.

The following parameters have been used for the processing of the QT database which is sampled at 250 Hz.

The sliding window $w = 32$, the smoothing window $p = 4$, the threshold for T-wave morphology test $\lambda = 6$. Denote $RR_i = R_{i+1} - R_i$, the search interval is chosen as

$$k_a = \begin{cases} R_i + \lfloor 0.15RR_i \rfloor + 37 & \text{if } RR_i < 220 \\ R_i + 70 & \text{if } RR_i \geq 220 \end{cases}$$

$$k_b = \begin{cases} R_i + \lceil 0.7RR_i \rceil - 9 & \text{if } RR_i < 220 \\ R_i + \lceil 0.2RR_i \rceil + 101 & \text{if } RR_i \geq 220 \end{cases}$$

where $\lfloor x \rfloor$ means the largest integer smaller than or equal to x, and $\lceil x \rceil$ means the smallest integer greater than or equal to x.

In order to evaluate the accuracy of the proposed algorithm, the mean and the standard deviation (STD) of the detection errors (the difference between the automatically detected T-wave ends and the manually annotated T-wave ends) are computed.

Up to our knowledge, the results of 4 different detection algorithms evaluated with the PhysioNet QT database have been published (Laguna et al., 1994), (Vila et al., 2000), (Martínez et al., 2004) and (Last et al., 2004). For the purpose of comparison, the results of the first 3 algorithms are recalled in Table 2. It has not been possible to compare with the results of (Last et al., 2004), because only 3000 annotated T-wave ends (out of 3542 available) were used for the results reported in this publication without indicating how these 3000 annotations were selected, and the mean value of the detection errors is not reported.

In Table 2, the first row (of numerical values) is the results with all the signals annotated by cardiologist 1, the other two rows are the results with the 11 records annotated by both cardiologists. Column 1 is the reference annotation used for error computation, column 2 is the number of records, column 3 is the number of annotated T-wave ends, column 4 is the results (mean and standard deviation (STD) of detection errors) of the proposed method, the

Reference	num. of records	num. of annot.	**this paper** mean	**this paper** STD	WT mean	WT STD	LPD mean	LPD STD	TU mean	TU STD
Cardio. 1	105	3542	**0.31**	**17.43**	-1.6	18.1	13.5	27.0	0.8	30.3
Cardio. 1	11	487	**-7.47**	**17.18**	-9.7	18.1	—	–	—	—
Cardio. 2	11	402	**-7.47**	**17.51**	-10.8	20.0	—	—	—	—

Table 2: Evaluation of algorithms on the QT database. The first row (of numerical values) is the results with all the signals annotated by cardiologist 1, the other two rows are the results with the 11 records annotated by both cardiologists. Column 1 is the reference annotation used for error computation, column 2 is the number of records, column 3 is the number of annotated T-wave ends, column 4 is the results (mean and standard deviation (STD) of detection errors) of the proposed method, the following columns are the results of the algorithms WT (Martínez et al., 2004), LPD (Laguna et al., 1994) and TU (Vila et al., 2000). The time unit is millisecond. The missing values are not reported in the original publication.

following columns are the results of the algorithms WT (Martínez et al., 2004), LPD (Laguna et al., 1994) and TU (Vila et al., 2000). The abbreviations for the names of these algorithms follow those of (Martínez et al., 2004). The time unit is millisecond. The numerical values for the algorithms WT, LPD, TU come from the publication (Martínez et al., 2004). The numerical values of the proposed method can be reproduced with the Matlab package (Zhang, 2005) which can be downloaded at http://www.irisa.fr/sosso/zhang/biomedical/.

In order to examine the robustness of the propose algorithm to baseline wander, the same signals are also processed without the filtering step. The results are similar to those obtained with filtered signals. For example, when evaluated with the 3542 annotations made by the first cardiologist, the mean of 0.018 millisecond and the standard deviation of 17.35 millisecond are obtained (to be compared respectively with the values of 0.31 and 17.43 obtained with filtered signals).

The computation of the mean and the standard deviation of errors needs some discussion. In Table 2, these values are computed according to the method adopted in (Martínez et al., 2004) as explained in the following.

- First, an algorithm is applied to each of the two leads of a ECG record in the QT database. *For each T-wave* annotated by cardiologist, the T-wave end is located twice by the algorithm, one per ECG lead. The *a posteriori* best result among the two computed positions is chosen for error evaluation. The explanation given in (Martínez et al., 2004) is that the cardiologist has made his annotation by looking at both leads and his decision is based on the best lead.

- Second, for each record, a mean value and a standard deviation of the T-wave end location errors are computed.

- Finally, the overall mean and standard deviation are computed for all the annotated 105 or 11 ECG records.

Reference	num. of records	num. of annot.	weighted mean	weighted STD	unique set mean	unique set STD
Cardio. 1	105	3542	0.38	18.05	1.72	41.27
Cardio. 1	11	487	-6.45	18.94	-3.22	26.41
Cardio. 2	11	402	-9.82	17.06	-9.84	29.32
Error Cardio.1-2	11	402	-5.84	24.46	-5.84	39.89

Table 3: Alternative algorithm evaluations. The "weighted" column: mean and standard deviation weighted by the number of annotations in each record, with the best lead selected per cardiac cycle. The "unique set" column: mean and standard deviation computed over all the errors in a unique set, with the best lead selected per record. The last row is the corresponding evaluation of the errors between the two cardiologists' T-wave end annotations. The time unit is millisecond.

How should the overall mean and standard deviation be computed? In (Martínez et al., 2004) the reported values (as recalled in Table 2) are simply taken as the mean of the mean values and the mean of the standard deviations. Though this detail has not been explicitly stated, but for the errors between the two cardiologists' T-wave end annotations, the reported mean value 2.1 and the standard deviation 22.4 have been clearly computed in this way.

A simple modification of the above scheme is to replace the mean (of mean values or standard deviations) by the mean *weighted* with the number of annotated T-wave ends in each record. The obtained values with the proposed algorithm is shown in Table 3 in the column indicated by "weighted". Another possibility is to collect the detection errors corresponding to all the annotated T-wave ends into a unique set and then compute a single mean and a single standard deviation over this set. In general the resulting standard deviation is larger than those computed with the previous schemes. The result obtained with the proposed algorithm is given in Table 3 in the column indicated by "unique set". Remark that, when this last result was computed, for each record of ECG signal, the best lead (out of the two) was chosen *once for the entire record* (in contrast to the choice per annotated T-wave end used in the previous schemes). In clinical practice, for each patient, the human operator can choose the best lead once when the ECG recorder is set up, but it is less reasonable to manually choose the best lead per cardiac cycle.

Before closing this section on numerical results, let us remark that, for the algorithm proposed in this paper, the T-wave end is always searched for in every cardiac cycle. As mentioned at the end of Section 2.4, the same algorithm could also be used to detect the presence of a T-wave in each cardiac cycle. Its application would eliminate some cardiac cycles annotated by the cardiologists. Since it is not possible to eliminate the same cardiac cycles as the other algorithms, the accuracy of T-wave end detection would have to be compared on different cardiac cycles. Eliminating "bad" cardiac cycles from the records generally improves the results. Therefore, evaluating the location errors on all the avail-

able manually annotated T-wave ends puts the proposed algorithm in the least favorable evaluation condition.

4 Conclusion

A new algorithm for T-wave end location has been presented in this paper. It is based on a indicator signal with mathematically proved consistency. It is robust to measurement noise, to T-wave morphological variations and to baseline wander. The computation burden of the algorithm is very low: its main computation can be implemented as a simple FIR filter.

Satisfactory results have been obtained when this new algorithm is evaluated on the PhysioNet QT database. In terms of error mean value and standard deviation, it outperforms the other algorithms evaluated on the same data base, according to recent publications.

By examining the errors of the algorithm, it has been observed that the large errors are mainly due to incorrect morphological classification. In order to further improve the result, it is important to develop more accurate and robust methods for morphological classification.

Appendix

Lemma 1 *Let $f(x)$ be an integrable function defined for $x \in [a,b]$ and denote*

$$\underline{f} = \min_{x\in[a,b]} f(x)$$

Assume that $f(x)$ satisfies the Lipschitz condition

$$|f(x) - f(x')| \leq M|x - x'| \quad \textit{for all} \quad x, x' \in [a,b]$$

with some constant $M > 0$. Then

$$\int_a^b [f(x) - \underline{f}]dx \leq \frac{1}{2}M(b-a)^2$$

Proof.
Denote

$$x_{\min} = \arg\min_{x\in[a,b]} f(x)$$

If the global minimum of $f(x)$ in $[a, b]$ is not unique, then take $x_{\min}$ as any of the minimizing value.

$$\begin{aligned}\int_a^b [f(x) - \underline{f}]dx &= \int_a^b |f(x) - f(x_{\min})|dx \\ &\leq \int_a^b M|x - x_{\min}|dx \\ &= -M\int_a^{x_{\min}} (x - x_{\min})dx + M\int_{x_{\min}}^b (x - x_{\min})dx \\ &= \frac{1}{2}M(a - x_{\min})^2 + \frac{1}{2}M(b - x_{\min})^2 \\ &= \frac{1}{2}M(b - a)^2 - M(x_{\min} - a)(b - x_{\min})\end{aligned}$$

By definition $x_{\min} \in [a, b]$, therefore $(x_{\min} - a)(b - x_{\min}) \geq 0$. Remind that $M > 0$. It is thus concluded that

$$\int_a^b [f(x) - \underline{f}]dx \leq \frac{1}{2}M(b - a)^2$$

Bibliography

Abboud, S. and Sadeh, D. (1984). The use of cross correlation function for the alignment of ECG waveforms and rejection of extrasystols. *Computers and Biomedical Research*, 17:258–266.

Goldberger, A. L., Amaral, L. A. N., Glass, L., Hausdorff, J. M., Ivanov, P. C., Mark, R. G., Mietus, J. E., Moody, G. B., Peng, C.-K., and Stanley, H. E. (2000). PhysioBank, PhysioToolkit, and PhysioNet: Components of a new research resource for complex physiologic signals. *Circulation*, 101(23):e215–e220. Circulation Electronic Pages: http://circ.ahajournals.org/cgi/content/full/101/23/e215.

Kohler, B.-U., Hennig, C., and Orglmeister, R. (2002). The principles of software QRS detection. *IEEE Engineering in Medicine and Biology Magazine*, 21(1):42 – 57.

Laguna, P., Jané, R., and Caminal, P. (1994). Automatic detection of wave boundaries in multilead ECG signals: Validation with the CSE database. *Computers and Biomedical Research*, 27:45–60.

Laguna, P., Mark, R. G., Goldberger, A., and Moody, G. B. (1997). A database for evaluation of algorithms for measurement of QT and other waveform intervals in the ECG. *Computers in Cardiology*, 24:673–676.

Last, T., Nugent, C. D., and Owens, F. J. (2004). Multi-component based cross correlation beat detection in electrocardiogram analysis. *BioMedical Engineering OnLine*, 3(26). http://www.biomedical-engineering-online.com/content/3/1/26.

Li, C., Zheng, C., and Tai, C. (1995). Detection of ECG characteristic points using wavelet transforms. *IEEE Transactions on Biomedical. Engineering*, 42(1):21–28.

Lindecrantz, K. G. and Lilja, H. (1988). New software QRS detector algorithm suitable for real time applications with low signal to noise ratio. *Journal of Biomedical Engineering*, 10:280–284.

Malik, M. and Camm, A. J. (1989). Computer model of cardiac repolarization processes and of the recovery sequence. *Computers and Biomedical Research*, 22(2):160–80.

Martínez, J. P., Almeida, R., Olmos, S., Rocha, A. P., and Laguna, P. (2004). A wavelet-based ECG delineator: Evaluation on standard database. *IEEE Trans. on Biomedical Engineering*, 51(4):570–581.

Moss, J., Schwartz, P., Crampton, R., Locati, E., and Carleen, E. (1985). The long QT syndrome: a prospective international study. *Circulation*, 71:17–21.

Padrini, R., Butrous, G., Camm, A. J., and Malik, M. (1995). Algebraic decomposition of the tu wave morphology patterns. *Pacing and Clinical Electrophysiology*, 18:2209–2215.

Schuartz, P. J. and Wolf, S. (1978). T interval prolongation as predictor of sudden death in patients with myocardial infarction. *Circulation*, 57:1074–1079.

Strumillo, P. (2002). Nested median filtering for detecting T-wave offset in ECGs. *Electronics Letters*, 38(14):682–683.

Vila, J., Gang, Y., Presedo, J., Fernández-Delgado, M., Barro, S., and Malik, M. (2000). A new approach for TU complex characterization. *IEEE Trans. on Biomedical Engineering*, 47(6):764–772.

Zhang, Q. (2005). Matlab package for robust and efficient location of T-wave ends in ECG and its evaluation with PhysioNet data. http://www.irisa.fr/sosso/zhang/biomedical/.